

**České vysoké učení technické v Praze
Fakulta stavební**

**Czech Technical University in Prague
Faculty of Civil Engineering**

Doc. Ing. Pavel Kuklík, CSc.

**Vliv strukturální pevnosti zeminy na interakci mezi stavbou
a podložím**

**Preconsolidation, Structural Strength of soil, and its effect on subsoil
upper structure interaction**

Summary

When constructing a building, manufactured materials are used. That is the reason of their excellent material properties. In the case of the foundation, the natural condition of the soils must be almost respected. The geostatical stress plays a significant role on the subsoil behavior because it is the de facto natural form of the soil compaction. The soil has a memory of the highest stress that has been ever loaded. The soil can be considered incompressible if the magnitude of a surcharge is lower. In engineering practice the construction of higher buildings is founded in a deeper hole so that the depth of the influence zone achieves an acceptable value for the future surcharge of the upper structure. For extremely tall buildings, the deep hole foundation must be prolonged by the piles. In particular, this article deals with laboratory testing that provides the preconsolidation. In Czech, we use the structural strength of soil. The test provides the initial void ratio and the initial coefficient of fully saturated hydraulic conductivity, as well. The isotropic consolidation test in triaxial test apparatus and consequent knowledge of the pore pressure course was chosen to determine the initial soil properties, including the preconsolidation level. Derived theory together with the genetic algorithms provides an efficient tool for the determining parameters. Good knowledge of the influence zone is crucial when solving soil structure interaction. The progress of the influence zone was considered from the extensive research carried out in the UnB Brasília. Thus, using the measurements, the preconsolidation and its effect were verified in situ. The derived formulas and presented graphs for influence zone depth estimation have considerable importance for civil engineering practice. The Kantorovich method together with the strategy of convolution was used to reach dimensional reduction when deriving analytical formulas. Recommended results and formulas were verified via FEM code ADINA.

Souhrn

Při realizaci vrchních staveb jsou zejména používány materiály speciálně vyráběné pro tyto účely, čemuž odpovídají i jejich výborné materiálové vlastnosti. V případě spodní stavby se tyto materiály dají využít jen omezeně. Musíme se smířit s tím, že o chování podloží a jeho materiálových vlastnostech již dříve rozhodla příroda. Vlastnosti podloží jsou zcela neodmyslitelně ovlivněny geostatickou napjatostí, což je de facto forma přírodního hutnění. Jestliže zatížení dosahuje menších hodnot, než na které byla struktura zeminy zhutněna, předkonsolidována, v českém jazyce se vžil termín strukturní pevnost zeminy, je její deformace prakticky zanedbatelná. V inženýrské praxi se toho využívá tak, že při stavbě vyšších objektů zakládáme v hlubších jamách tak, aby deformační zóna dosahovala přípustné hloubky a deformace podloží vlivem přitížení byla pro vrchní stavbu přijatelná. Pro mimořádně vysoké budovy, kdy stavební jámy by byly v daných hloubkách nerealizovatelné, se „spouštíme“ k nejúnosnějším vrstvám prostřednictvím pilot. Předkládaný příspěvek se zabývá mimo jiné laboratorním stanovením strukturní pevnosti zeminy, předkonsolidace, stanovením počátečního čísla pórovitosti a počáteční nasycené hydraulické vodivosti. Ke stanovení počátečních vlastností zeminy byl použita znalost vývoje pórových tlaků v průběhu isotropní konsolidace v triaxiálním přístroji. Odvozená teorie spolu s technikou genetických algoritmů poskytuje účinný sofistikovaný aparát k určování zmíněných skutečností. Při řešení problematiky interakce vrchní stavba - podloží je důležitá znalost hloubky deformační zóny pod základem. K ověření vývoje hloubky deformační zóny byly využity rozsáhlé výzkumy provedené na UnB Brasílii. Na základě odvozených teorií byly strukturní pevnost zeminy a vliv deformační zóny validovány in situ. Značný význam pro stavební praxi mají odvozené vzorce a grafy sloužící k rychlému odhadu deformační zóny. Při odvozování analytických vzorců byla k dimensionální redukci použita Kantorovičova metoda posílená a strategii konvolucí. Odvozené vzorce byly verifikovány prostřednictvím MKP kódem ADINA.

Klíčová slova: deformační zóna, předkonsolidace, strukturální pevnost, MKP, triaxiální zkouška, polní zkoušky, hluboké základy, vrstevnaté podloží, modifikovaný Cam clay, Kantorovičova metoda, teorie konvolucí

Keywords: Influence zone, Preconsolidation, Structural strength, FEM, Triaxial test, In situ testing, Deep foundation, Layered subsoil, Modified Cam clay model, Kantorovich method, theory of convolution

Contents

1. Introduction	6
2. Preconsolidation, structural strength, in laboratory testing	6
3. Verification of preconsolidation in situ and its testing	12
4. Elastic layer theory, basic ideas of dimensional reduction	19
5. The phenomenon of influence zone and its estimation	23
6. FEM validation of derived formulas	28
7. Conclusion	30

1 Introduction

It has been experimentally confirmed that a soil substantially changes its material properties when subjected to external loading. Apart from that, the soil, when subjected to a certain loading history, has the ability to memorize the highest level of loading mathematically represented by the over-consolidation ratio, and initial void ratio. In its virgin state, the soil deformability is relatively high. On the contrary, following the unloading/reloading path shows almost negligible deformation until the highest stress state the soil has experienced ever before is reached [1], [2], and [21]. To study this behavior of soil, we performed several small laboratory tests. Transport processes were observed carrying out isotropic consolidation in triaxial test apparatus. Employing genetics algorithms, soil parameters were determined comparing the pore pressure course (measured and calculated) [9], [17]. In large scale, the effect of over consolidation was simultaneously investigated by way of rigid plate and piles working diagrams analysis. Both the finite element technique and elastic layer theory were employed in back analysis of the measured data. The great effect of overburden was observed on the depth of the influence zone in deep hole foundations [12], [13]. This study is in general focused on the description of preconsolidation effects by self weight of overburden and on selection of the main parameters characterizing this memory of the subsoil.

2 Preconsolidation, structural strength, in laboratory testing

The test was arranged in two runs, loading/reloading. Readings were taken of the highest level of effective mean stress. Referring to experimental measurements carried out in the triaxial apparatus, the isotropic consolidation can be viewed as one phase flow in a fully saturated deforming medium undergoing small deformation. When neglecting the body forces, the hydrostatic state of stress maintained during the experimental measurement gives

$$\sigma_x(x, y, z, t) = \sigma_y(x, y, z, t) = \sigma_z(x, y, z, t) = \sigma_m(t), \quad (1)$$

where σ_m is the total mean stress. Following the Terzaghi-Fillunger concept of effective stresses, this quantity can be expressed in terms of the pore pressure p^s and the effective stresses between grains σ_m^{eff} as

$$\sigma_m = \sigma_m^{eff} - p^s. \quad (2)$$

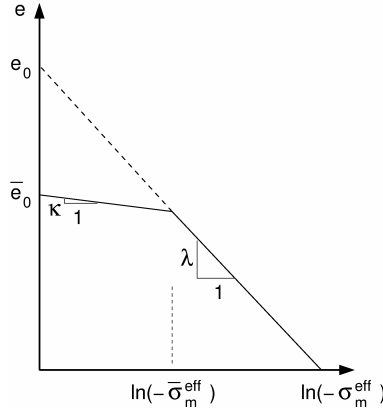


Figure 1: Bilinear form of the normal consolidation line

Assuming full saturation ($S_w = 1$) the pore pressure p^s equals the pressure in the liquid phase p^w . Referring to experimental conditions, the total mean stress remains constant throughout the consolidation process. The assumed stress homogeneity together with Eq. (2) then provide

$$\dot{\sigma}_m = \dot{\sigma}_m^{eff} - \dot{p}^w = 0, \quad (3)$$

where $(\dot{\quad})$ represents the time derivative $\partial(\quad)/\partial t$. Transport of the liquid phase throughout the soil sample can be described by the following set of equations:

Transport equation

$$J^w = -\frac{K \rho^w}{\gamma^w} \cdot \text{grad } p^w, \quad (4)$$

where J^w is the mass flux of pore water, $\gamma^w = g\rho^w$ is the specific weight of water, ρ^w is the intrinsic mass density and K represents an instantaneous coefficient of permeability.

Balance equation reads

$$\rho^w \dot{\epsilon}_v + \text{div } J^w = 0. \quad (5)$$

The volumetric strain ε_V follows from the

Constitutive equation

$$\varepsilon_V = \frac{e(t) - \bar{e}_0}{1 + \bar{e}_0} = -\frac{\kappa}{1 + \bar{e}_0} \ln(-\sigma_m^{eff}(t)),$$

$$\sigma_m^{eff} > \bar{\sigma}_m^{eff} = -p_c, \quad (6)$$

$$\varepsilon_V = \frac{e(t) - e_0}{1 + e_0} = -\frac{\lambda}{1 + e_0} \ln(-\sigma_m^{eff}(t)),$$

$$\sigma_m^{eff} < \bar{\sigma}_m^{eff} = -p_c, \quad (7)$$

they were derived for the case of the modified Cam clay model from the bilinear consolidation line, Fig. 1. The initial branch, often referred to as κ -line, gives evidence of the previous stress history and represents the effect of preconsolidation. The slope discontinuity between the κ and λ -lines can be identified with the structural strength of the soil given in terms of a certain level of the effective mean stress $\bar{\sigma}_m^{eff} = -p_c$ (p_c is termed the preconsolidation pressure).

Differentiating Eq. (7) with respect to time gives the rate of volumetric strain in the form

$$\dot{\varepsilon}_V(t) = \frac{\dot{e}(t)}{1 + e_0} = -\frac{\lambda}{1 + e_0} \frac{\dot{p}^w(t)}{\sigma_m^{eff}(t)}. \quad (8)$$

Substituting Eqs. (4) and (8) into Eq. (5) and taking into account the actual triaxial set-up, in which only the bottom face of the cylinder is drained, lead to

$$-\frac{1 + e_0}{\gamma^w \lambda} \sigma_m^{eff}(t) \frac{\partial}{\partial z} \left(K(t) \frac{\partial p^w(t)}{\partial z} \right) - \dot{p}^w(t) = 0. \quad (9)$$

It has been validated experimentally that in the case of isotropic consolidation a mere power law written as (more in [6], [9], and [11])

$$\frac{K(t)}{K_0} = \left(\frac{e(t)}{e_0} \right)^m, \quad (10)$$

represents the soil behavior fairly well. The dependence of the actual void ratio e on the effective mean stress, Eq. (7), together with Eq. (10) provide

$$\frac{\partial K(t)}{\partial z} = - \frac{mK(t)\lambda}{e(t)\sigma_m^{eff}(t)} \frac{\partial p^w(t)}{\partial z}. \quad (11)$$

Introducing Eq. (11) into Eq. (9) finally yields.

$$\begin{aligned} \dot{p}^w(t) = \\ = - \frac{K(t)(1+e_0)}{\gamma^w \lambda} \left[- \frac{m\lambda}{e(t)} \left(\frac{\partial p^w(t)}{\partial z} \right)^2 + \sigma_m^{eff}(t) \frac{\partial^2 p^w(t)}{\partial z^2} \right] \end{aligned} \quad (12)$$

a similar equation can be derived for the unloading branch when replacing λ by κ and e_0 by \bar{e}_0 in Eq. (12)

$$\begin{aligned} \dot{p}^w(t) = \\ = - \frac{K(t)(1+\bar{e}_0)}{\gamma^w \kappa} \left[- \frac{m\kappa}{e(t)} \left(\frac{\partial p^w(t)}{\partial z} \right)^2 + \sigma_m^{eff}(t) \frac{\partial^2 p^w(t)}{\partial z^2} \right]. \end{aligned} \quad (13)$$

The main objective of these steps is to introduce a simple yet accurate numerical technique for extracting material parameters of clayey soils that behave according to the Cam clay model, from a simple one-dimensional consolidation test. To introduce this task, recall that reproducing laboratory data requires supplying the structural strength parameter p_c , the initial void ratio \bar{e}_0 , the initial coefficient of permeability K_0 , the swelling index κ and the compression index λ . The last two material parameters and the starting value of preconsolidation pressure could be specified from the steady state response corresponding to the diagram shown in Fig. 1. This however, would require carrying out a number of isotropic

consolidation tests for several predefined levels of isotropic pressures attained at the end of the consolidation process while measuring at the same time the change in volumetric strain $\Delta\varepsilon_v$. Such an approach would become not only time consuming but also would be burdened by an additional experimental error associated with the difficulty of measuring $\Delta\varepsilon_v$ and the determination of \bar{e}_0 and K_0 would require additional laboratory tests. In addition a trial and error method would have to be used to determine the remaining parameter m .

A simple solution avoiding such difficulties is offered by following the steps of mixed experimental and numerical methods. In such a case, combining the experimental measurements and numerical computations in a suitable optimization environment provides an efficient tool for inferring the desired parameters from a single laboratory test. In particular, matching experimentally obtained data with those derived numerically might be the simplest view at a complex optimization procedure that provides the desired results.

To that end, recall Eq. (12) describing the excess pore pressure variation during consolidation. In view of the optimization problem, the used material and structural strength parameters ($\bar{e}_0, K_0, \kappa, \lambda, p_c, m$) now become the search variables to be found by minimizing the following function

$$F = \sum_{k=1}^{\kappa} (p^w(t_k) - \bar{p}^w(t_k))^2 .$$

In keeping up with the general scheme of the paper, we will limit our attention to two essential parameters, namely the preconsolidation pressure p_c representing the loading history and the exponent m affecting the time variation of the coefficient of permeability, Eq. (10) (details in [11], [17]).

To derive a robust numerical procedure, the optimal parameters were sought comparing numerical data with measured values of pore pressure. Example of result is listed bellow in Tab. 1.

Table 1: Optimal material parameters

κ [kPa]	λ [kPa]	e_0	K_0	p_c [kPa]	m
0.012	0.074	0.56	1.53 e^{-9}	28.45	4.7

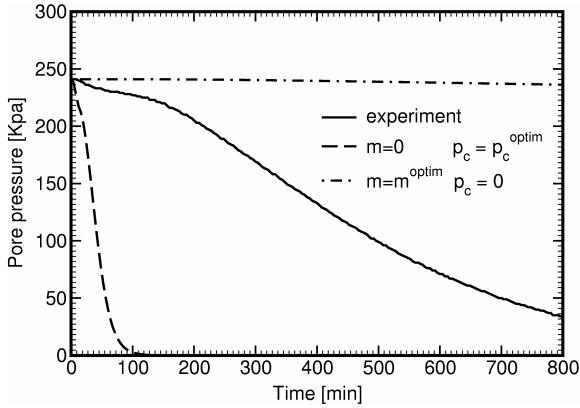


Figure 2: Time variation of pore pressure

An influence of the preconsolidation p_c and influence of the parameter m , describing the change of the permeability coefficient, are clearly presented in Fig. 2

Finally, the proposed theory is highlighted in Fig. 3. It is seen, that theoretical and measured loading/reloading curves fit fairly well (all details in [9]).

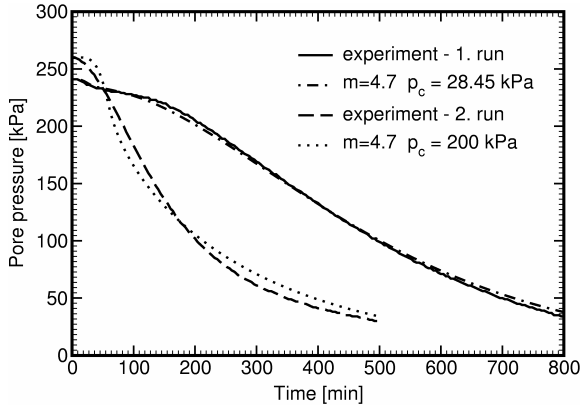


Figure 3: Time variation of pore pressure

3 Validation of preconsolidation in situ and its testing

The pre-designed Brazilian capital Brasília, located in the Federal District of Brazil, was designed to house only the main Governmental administrative institutions and its public employees. Nevertheless, it has

increased four times more than what was initially forecasted and is still expanding. Construction is advancing through distinct (geological) zones of this same district, and allowing the use of distinct techniques for deep foundation deployment and design.

Hence in 1995, the University of Brasília started a major research project, in order to enhance the knowledge on the behavior of the typical deep foundations that are founded in the stratified, tropical subsoil of the Federal District. It was decided to carry out horizontal and vertical field loading tests on locally used foundation types. These foundations had full-scale dimensions and were placed within the University of Brasília campus at the experimental research site of the Geotechnical Post-Graduation Program. The geotechnical profile of this campus is composed by the typical unsaturated “porous” clay of Brasília. In addition, field loading tests on full-scale instrumented foundations outside campus were also carried out. In all cases, the tests were performed with the cooperation of local engineering companies and University staff.

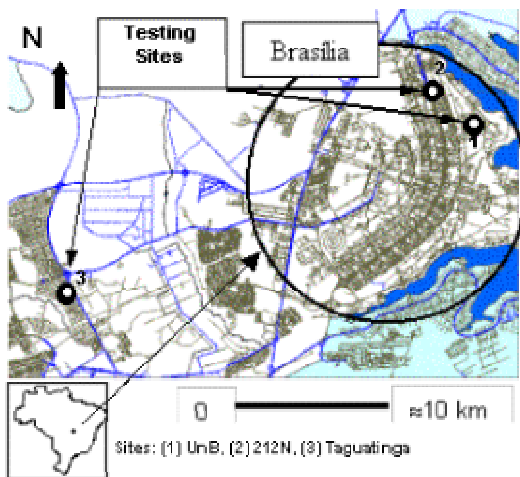


Figure 4: Location of the Studied Sites.

A mechanically bored pile founded in the University of Brasília campus (UnB research site) is analyzed together with instrumented piles from two other engineering sites within this same District. One of them is a continuous flight auger type pile located in the North Wing of Brasília (212N site), close to the University Campus, and founded in the same geological material. The other is a mechanically bored pile excavated with bentonite mud, located in a site around 25 km from the University

Campus (Taguatinga site), and founded in a foliated and stratified material which originates from slate decomposition.

The experimental curves of pile load versus displacement, structural load transfer along the pile's shaft, and average skin friction and base pressure versus loading level are presented and compared to numerical predictions from a semi-analytical procedure. This procedure is coded in the industrial software denominated GEO4 Pile modulus that was developed in cooperation between the Department of Mechanics, Faculty of Civil Engineering, CTU in Prague and Fine Ltd. Software Company.

Table 2: General Geotechnical Parameters of the UnB Site (Cunha et al. 1999).

Parameter	Unit	Range
Sand percentage	%	12-27
Silt percentage	%	8-36
Clay percentage	%	80-37
Dry unit weight	kN/m ³	10-17
Natural unit weight	kN/m ³	17-19
Moisture content	%	20-34
Degree of saturation	%	50-86
Void ratio	--	1.0-2.0
Liquid limit	%	25-78
Plastic limit	%	20-34
Plasticity index	%	5-44
Drained cohesion ^a	kPa	10-34
Drained Friction angle ^a	degrees	26-34
Young's Modulus ^b	MPa	1-8
Coefficient of Collapse	%	0-12
Coeff. Earth Press (K0) ^c	--	0.44-0.54
Coeff. Permeability	cm/s	10 ⁻⁶ -10 ⁻³

OBSERVATIONS:

- a- Triaxial CK0D tests-Inundated Soil and at natural humidity;
- b- Triaxial CK0D tests: Soil at natural humidity-50% failure deviator stress;
- c- Triaxial K0 tests: Soil at natural humidity.

The results of back analysis are depicted in Fig. 5 and Fig. 6. The necessity for a further refinement for both 212N and Taguatinga analyses is evident when comparing the load transfer curves of these same sites, as respectively done in Fig. 7 and Fig. 8. Hence, although refinement is required, the results can be already considered suitable from a practical point of view, if one

accepts as valid and within tolerable range (in engineering terms) the errors involved in this first series of analyses.

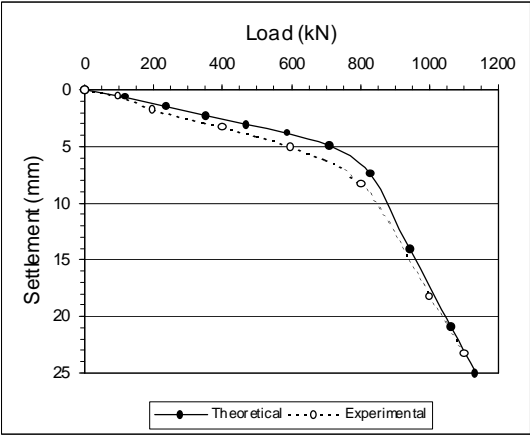


Figure 5: Load-Displacement Curve Obtained for the 212N Pile

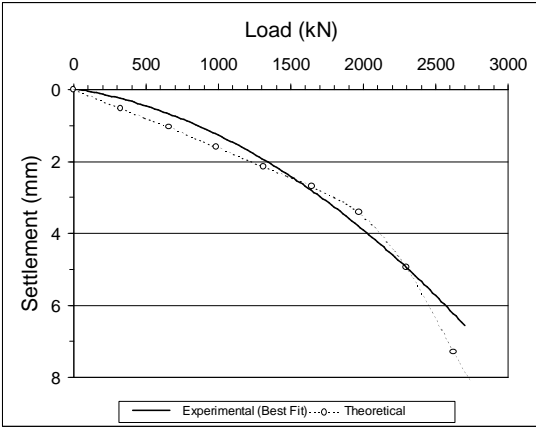


Figure 6: Load-Displacement Curve Obtained for the Taguatinga Pile.

Table 3: Back analyzed Geotechnical Parameters from All Sites via GEO4 Software.

Sublayer Type	Depth (m)	Geotechnical Parameter				N [*] _(SPT)
		ϕ' (deg)	c' (kPa)	E (MPa)	K	
<u>UnB Site:</u>						
Clay I	0-3	27	13	5	0.6	3
Clay II	3-8	27	14	13	0.6	4
Clay III	8-12	27	52	19	0.6	4-15
Rock	> 12 (Non Deformable)					
<u>212N Site:</u>						
Embankment	0-4	25	0	25	0.4	9
Clay A	4-8	27	15	20	0.4	9-5
Clay B	8-15	27	5	40	0.4	5-15
Clay C	15-25	27	5	100	0.4	15-20
Rock	> 25 (Non Deformable)					
<u>Taguatinga Site:</u>						
S Clay	0-2.5	27	15	20	0.7	6
CSand	2.5-5	30	10	60	0.7	10
SSilt I	5-10	30	20	120	0.7	16-40
SSilt II	10-15	40	30	600	0.7	50+
Rock	> 15 (Non Deformable)					

OBSERVATIONS: (*) Average estimated values based on few, non-statistical, results

ϕ' = Effective Friction Angle; c' = Effective Cohesion; E = Young Modulus; γ = Apparent Unit Weight;

ν_{soil} = Poisson Coefficient = 0.3; K = Coeff. of Earth Pressure; γ_{soil} = 16.5 kN/m³

Structural Parameters: E = 20000 MPa (UnB, 212N) and 30000 MPa (Taguatinga), γ_{concrete} = 25 kN/m³

Figure 8 presents the comparison of load transfer curves for the Taguatinga pile. It indicates that a fairly good result was obtained, and a better (than 212N pile) agreement was achieved. Similarly as before, one can affirm that the analyses can be already considered as valid from a practical point of view. Indeed, the comparison of average unit skin friction and percentage of base load between numerical and experimental values is good. It is observed that, for the failure condition (3200 kN), $\approx 42\%$ of the applied load at the pile's head was transmitted to the base of this pile (numerical prediction).

At working condition (1600 kN) however, the software has estimated that $\approx 11\%$ of the applied load at the pile's head would be transmitted to the base of this pile. Also at this latter condition, the comparison of average unit skin friction between numerical (≈ 56 kPa) and experimental (≈ 40 kPa) values was reasonably good.

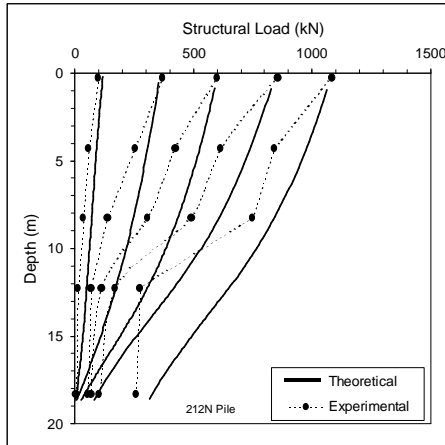


Figure 7: Load Transfer Curve – 212N Pile.

This value is very close to the value that has been experimentally measured throughout the test (as given before, in the range of 40%).

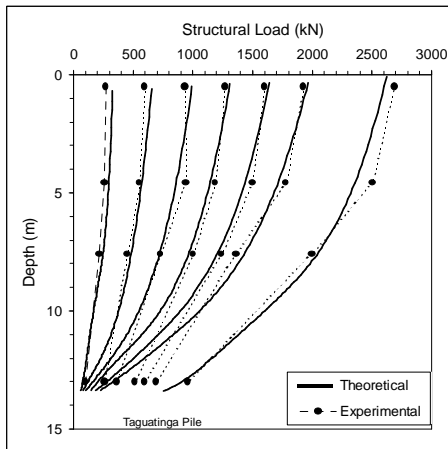


Figure 8: Load Transfer Curve - Taguatinga Pile.

The discrepancies are again related to the fact that the pile was founded in a very hard soil stratum (saprolite), which was not perfectly simulated in this first analysis.

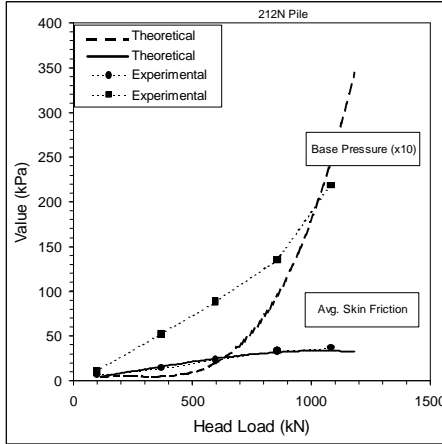


Figure 9: Comparative Results for the 212N Pile.

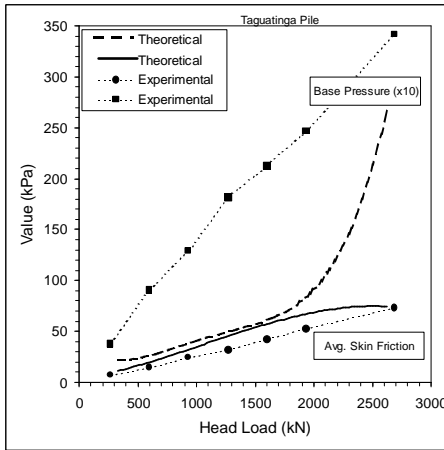


Figure 10: Comparative Results for the Taguatinga Pile.

The lack of agreement for the base pressure is directly related to the fact that the analyses lacked to properly model the last layer or the foundation layer, where extremely high values of unit pressures took place and were indirectly measured. In numerical terms, a unique and particular soil spring was assigned to this last layer. Since it is evident from Figs. 9 and 10 (in particular the latter one) that the numerically predicted base pressures

were substantially lower than the measured values, one can conclude that the stiffness of this spring was not properly incorporated in the analyses. A fine readjustment of the stiffnesses for both situations, increasing towards more representative values, would certainly improve the matching quality of the load transfer curves of Fig. 9 and Fig. 10, especially at the deepest pile sections.

The experience gained with these analyses has demonstrated that a deep strata, stiffer than the overlying layers and leveled to the pile's base, shall be incorporated in the numerical back analysis. This holds particularly true for the Taguatinga site, where the pile was founded on a hard saprolite medium. It was also learned of the importance of having instrumented piles at the site. Although such efforts may increase construction costs, the assistance of the instrumentation in guiding and benchmarking the back analysis is immeasurable (more information in [3], [4]).

4 Elastic layer theory, basic ideas of dimensional reduction

The aim of the analytical solution is to determine the deformation of an elastic layer in the vertical direction. The solution procedure builds upon neglecting the horizontal displacements similar to standard assumptions applied to the analysis of Westergard subspace. Clearly, such an assumption results in a stiffer soil response thereby providing an upper estimation of the depth of influence zone. The problem formulation is evident from Fig. 11. Referring to the Kantorovich method (details in [19], [20]) the distribution of the displacement field is obtained in the form

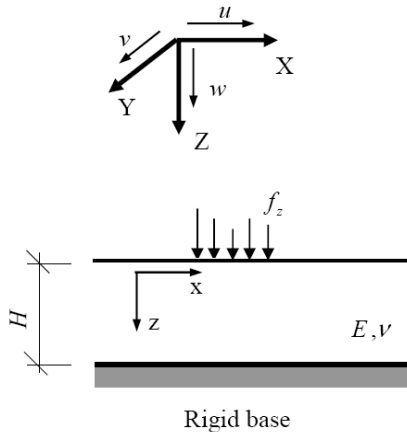


Figure 11: Formulation of the elastic layer solution

$$w(x; y; z) = \sum_{j=1,3,5}^{\infty} w_j(x; y) \psi_j(z), \quad (14)$$

$$\psi_j(z) = \cos \frac{j\pi}{2H} z,$$

where the functions $\psi_j(z)$, $j=1,3,5,\dots$ represent a complete set of base functions. Let us calculate the components of the small strain tensor. The small strain tensor is the symmetrical part of the gradient matrix tensor. From (14), it yields:

$$\varepsilon_{xx} = 0, \quad \varepsilon_{yy} = 0, \quad \varepsilon_{zz} = \sum_{j=1,3,5}^{\infty} w_j \psi_{j,z}, \quad (15)$$

$$\gamma_{xy} = 2\varepsilon_{xy} = 0, \quad \gamma_{yz} = 2\varepsilon_{yz} = \sum_{j=1,3,5}^{\infty} w_{j,y} \psi_j, \quad \gamma_{zx} = 2\varepsilon_{zx} = \sum_{j=1,3,5}^{\infty} w_{j,x} \psi_j.$$

Notation $\frac{\partial w_j}{\partial x} = w_{j,x}$ is used for the partial derivative.

For the stress-strain relation, Hooke's law is adopted:

$$\sigma_{xx} = \frac{\nu}{1-\nu} E_{oed} \sum_{j=1,3,5}^{\infty} w_j \psi_{j,z}, \quad \sigma_{yy} = \frac{\nu}{1-\nu} E_{oed} \sum_{j=1,3,5}^{\infty} w_j \psi_{j,z}, \quad \sigma_{zz} = E_{oed} \sum_{j=1,3,5}^{\infty} w_j \psi_{j,z}, \quad (16)$$

$$\tau_{xy} = G\gamma_{xy} = 0, \quad \tau_{yz} = G \sum_{j=1,3,5}^{\infty} w_{j,y} \psi_j, \quad \tau_{zx} = G \sum_{j=1,3,5}^{\infty} w_{j,x} \psi_j.$$

Symbols E, ν, E_{oed}, G represent known values of Young's modulus, Poisson's ratio, oedometric modulus and shear modulus, respectively. Lagrange's principle of virtual work as the general principle of equilibrium is used in the following form:

$$\int_{R^2} \left(\int_0^H \left(G \frac{\partial w}{\partial x} \frac{\partial \delta w}{\partial x} + G \frac{\partial w}{\partial y} \frac{\partial \delta w}{\partial y} + E_{oed} \frac{\partial w}{\partial z} \frac{\partial \delta w}{\partial z} \right) dz - f_z(x, y) \delta w(x, y, 0) \right) dx dy = 0. \quad (17)$$

Since the virtual functions δw will be used in the same form as w , integrating the equilibrium equation in the vertical direction takes the form of an infinite number of partial differential equations:

$$-\Delta w_j(x, y) + (j\alpha)^2 w_j(x, y) = \frac{2}{GH} f_z(x, y), \quad j=1,3,5,\dots, \quad (18)$$

$$\alpha = \frac{\pi}{2H} \sqrt{\frac{E_{oed}}{G}} = \frac{\pi}{2H} \sqrt{\frac{2-2\nu}{1-2\nu}}.$$

In the case of axisymetry or if the uniform load is acting on infinite strip, the solution can be searched by solving the system of ordinary differential equations. Otherwise, the strategy of convolution must be employed. Eq. (18) is the generalized form of the known Pasternak solution of subsoil (see e.g. [5], [7], [10], [18])

The solution of the partial differential equation can be written as the convolution of the right hand side and the fundamental solution F_j corresponding to the left hand side

$$\begin{aligned} w_j(x, y) &= \frac{2}{GH} \int_{R^2} f_z(\xi, \eta) F_j(\xi - x, \eta - y) d\xi d\eta = \\ &= \frac{2f_z}{GH} \int_{R^2} F_j(\xi - x, \eta - y) d\xi d\eta \end{aligned} \quad (19)$$

The function F_j satisfies the equation

$$-\Delta F_j + (j\alpha)^2 F_j = 0 \quad \text{for } x^2 + y^2 > 0 \quad (20)$$

It is of the form

$$F_j = \frac{1}{2\pi} K_0(j\alpha\sqrt{x^2 + y^2})$$

where $K_0(j\alpha\sqrt{x^2 + y^2})$ is the modified Bessel function of zero order (see [8], [19]). Due to singularity of F_j at $[0,0]$ satisfies the right hand side of (19) is evaluated as the limit of integrals over the smaller region $\Omega_\varepsilon = \Omega \setminus K_\varepsilon$ for $\varepsilon \rightarrow 0$, where K_ε is the small ball of a small positive radius ε and the center at the point $[x, y]$. Integrating (20) over and applying Green's theorem we can write

$$\begin{aligned} \int_{\Omega_\varepsilon} F_j(\xi - x, \eta - y) d\xi d\eta &= \frac{1}{(j\alpha)^2} \int_{\Omega_\varepsilon} \Delta F_j(\xi - x, \eta - y) d\xi d\eta = \\ &= \frac{1}{(j\alpha)^2} \oint_{\partial\Omega_\varepsilon} \left(\frac{\partial F_j}{\partial \xi} d\eta - \frac{\partial F_j}{\partial \eta} d\xi \right). \end{aligned} \quad (21)$$

If $[x, y]$ is not a point of $\partial\Omega$, $\partial\Omega \setminus K_e = \partial\Omega$, in particular we can simplify and write

$$w_j(x, y) = \frac{2f_z}{GH} \left(\frac{1}{j\alpha} \right)^2 \left(1 + \oint_{\partial\Omega} \left(\frac{\partial F_j}{\partial \xi} d\eta - \frac{\partial F_j}{\partial \eta} d\xi \right) \right), \quad (22)$$

for $[x, y] \in \Omega$,

$$w_j(x, y) = \frac{2f_z}{GH} \left(\frac{1}{j\alpha} \right)^2 \oint_{\partial\Omega} \left(\frac{\partial F_j}{\partial \xi} d\eta - \frac{\partial F_j}{\partial \eta} d\xi \right), \quad (23)$$

for $[x, y] \in R^2 \setminus (\Omega \cup \partial\Omega)$.

If $w_j(x, y)$ for $j = 1, 3, 5, \dots$ are known functions, the stress function $\sigma_{zz}(x, y, z)$ takes the form

$$\sigma_{zz}(x, y, z) = -E_{oed} \frac{\partial w}{\partial z}(x, y, z) = E_{oed} \sum_{j=1,3,\dots} \frac{j\pi}{2H} w_j(x, y) \sin\left(\frac{j\pi z}{2H}\right) \quad (24)$$

5 The phenomenon of influence zone and its estimation

We introduce the subject considering the distribution of vertical stresses according to Fig. 12. Due to excavation to a certain depth h , the original geostatic stress state, which sets the initial compaction of soil represented by the preconsolidation pressure (see [16]), the highest stress level in the soil recorded during the prior loading history, is reduced. Subsequent surcharge at the footing bottom gives further redistribution of the vertical stress. It is assumed that in the region where the vertical effective stress due to surcharge at the footing bottom combined with the reduced geostatic effective stress (by excavation) does not exceed the original geostatic effective stress, the skeleton deformations are negligible. This condition, in our sense, describes the depth of the influence zone H ([5], [12]).

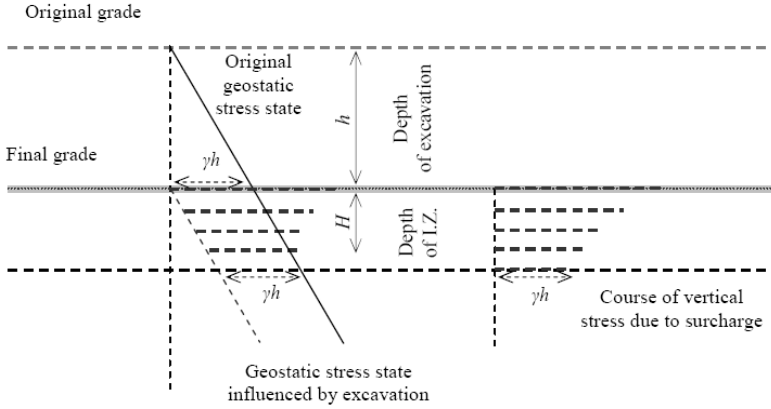


Figure 12: The governing idea of the influence zone calculation

Denote the width of uniform load strip f_z by $2a$, i.e. $\Omega = \{[x, y]: -a < x < a, y \in R\}$. The solution $w(x, y, z)$ of (18) is independent on y : $w = w(x, z)$. There are an infinite number of the ordinary differential equations, together with the boundary and continuity conditions

$$\lim_{|x| \rightarrow \infty} w_j(x) = 0, \quad w_j \in C^1(R), \quad j = 1, 3, \dots$$

produces the solution

$$w_j(x) = \begin{cases} A_0 + A_1 \cosh(j\alpha x) & \text{for } x \in (-a, a) \\ A_2 \exp(-j\alpha|x|) & \text{for } |x| > a, \end{cases}$$

$$\text{where} \quad A_0 = \frac{2f_z}{GH} \left(\frac{1}{j\alpha} \right)^2.$$

Unknown constants A_1, A_2 of integration result from the condition of continuity (of the displacement and its first derivative) in the points of $|x| = a$. Inserting these constants into above formula it provides

$$w_j(x) = \frac{2f_z}{GH} \left(\frac{1}{j\alpha} \right)^2 \cdot \begin{cases} 1 - \cosh(j\alpha x) \exp(-j\alpha a) & \text{for } |x| \leq a \\ \exp(-j\alpha|x|) \sinh(j\alpha a) & \text{for } |x| > a. \end{cases} \quad (25)$$

Hence, the function $w(x, z)$ being in the form of series

$$w(x, z) = \sum_{j=1,3,\dots} w_j(x) \cos\left(\frac{j\pi z}{2H}\right) \quad (26)$$

solves the problem. The component of the vertical stress function σ_{zz} is evaluated by differentiating $w(x, z)$ with respect to z by terms

$$\begin{aligned} \sigma_{zz}(x, z) &= -E_{oed} \frac{\partial w}{\partial z}(x, z) = E_{oed} \sum_{j=1,3,\dots} \frac{j\pi}{2H} w_j(x) \sin\left(\frac{j\pi z}{2H}\right) = \\ &= \frac{4f_z}{\pi} \sum_{j=1,3,\dots} \frac{1}{j} \sin\left(\frac{j\pi z}{2H}\right) \begin{cases} 1 - \cosh(j\alpha x) \exp(-j\alpha a) & \text{for } |x| \leq a \\ \exp(-j\alpha|x|) \sinh(j\alpha a) & \text{for } |x| > a. \end{cases} \end{aligned}$$

All three series in the above formula can be summed (more in [8]). Finally, the vertical stress σ_{zz} can be written in the form

$$\sigma_{zz}(x, z) = f_z - \frac{f_z}{\pi} \left(\arctan\left(\frac{\sin(\pi z / 2H)}{\sinh(\alpha(a-x))}\right) + \arctan\left(\frac{\sin(\pi z / 2H)}{\sinh(\alpha(a+x))}\right) \right), \quad \text{for } |x| \leq a \quad (27)$$

$$\sigma_{zz}(x, z) = \frac{f_z}{\pi} \left(\arctan\left(\frac{\sin(\pi z / 2H)}{\sinh(\alpha(|x|-a))}\right) - \arctan\left(\frac{\sin(\pi z / 2H)}{\sinh(\alpha(|x|+a))}\right) \right), \quad \text{for } |x| > a.$$

The stress function $\sigma_{zz}(x, z)$ for fixed $z \in \langle 0, H \rangle$ acquires its maximum at the point $x = 0$:

$$\begin{aligned} \max_{x \in R} \sigma_{zz}(x, z) &= \sigma_{zz}(0, z) = f_z - \frac{2f_z}{\pi} \arctan\left(\frac{\sin(\pi z / 2H)}{\sinh \alpha a}\right) = \\ &= \frac{2f_z}{\pi} \arctan\left(\frac{\sinh \alpha a}{\sin(\pi z / 2H)}\right). \end{aligned}$$

The function $\sigma_{zz}(0, z)$ decreases with increasing z . The maximum of the stress function at the bottom ($z=H$) of the influence zone depth is

$$\sigma_{zz}(0, H) = \frac{2f_z}{\pi} \arctan \sinh \alpha a. \quad (28)$$

The influence zone depth is estimated by means of the quality

$$\sigma_{zz}(0, H) = \gamma h, \quad (29)$$

where γ is the specific weight of soil and h is the depth of the excavation. Comparing the last two identities we obtain

$$\frac{\gamma h}{f_z} = \frac{2}{\pi} \arctan \sinh \alpha a.$$

Denoting

$$\beta = \frac{2\alpha a}{\pi} = \frac{a}{H} \sqrt{\frac{2-2\nu}{1-2\nu}}, \quad F_{strip}(\beta) = \frac{2}{\pi} \arctan \left(\sinh \frac{\beta\pi}{2} \right).$$

The above identities give the equation

$$\frac{\gamma h}{f_z} = F_{strip}(\beta).$$

Eliminating the influence zone finally yields

$$\begin{aligned} H &= \frac{\pi a}{2} \sqrt{\frac{2-2\nu}{1-2\nu}} \frac{1}{\sinh^{-1} \left(\tan \frac{\pi \gamma h}{2 f_z} \right)} = \frac{\pi(2a)}{4} \sqrt{\frac{2-2\nu}{1-2\nu}} \frac{1}{\sinh^{-1} \left(\tan \frac{\pi \gamma h}{2 f_z} \right)} = \\ &= \frac{\pi a}{2} \sqrt{\frac{2-2\nu}{1-2\nu}} \frac{1}{\ln \left(\sin \frac{\pi \gamma h}{2 f_z} + 1 \right) - \ln \left(\cos \frac{\pi \gamma h}{2 f_z} \right)}. \end{aligned} \quad (30)$$

This closed formula can be effectively used in civil engineering practice. Now we give several comments on the derived identity. First, the influence zone is proportional to the strip load width $2a$. Secondly, the influence zone doesn't depend on Young's modulus, but there is a significant role for Poisson's ratio. Overloading of the excavation geostatic stress state $f_z / \gamma h$ is the third parameter to be taken into account. All these statements are highlighted in the following Fig. 13.

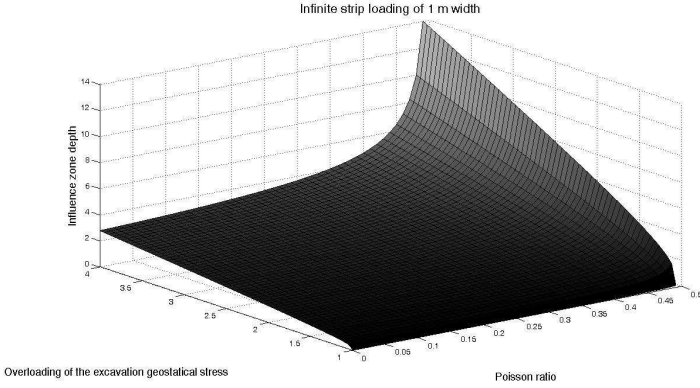


Figure 13: Progress of influence zone depth of the 1m wide strip

Similarly, we can estimate the depth of influence zone in the case of rectangular footings. Let us introduce the function

$$\begin{aligned}
 F(\beta) = & \frac{2}{\pi} \left(\arctan \frac{\beta \pi b}{2a} + \arctan \frac{\beta \pi}{2} \right) - \\
 & - \frac{4}{\pi^2} \int_0^1 \frac{1}{\sqrt{\left(\frac{a}{b}\right)^2 + 1 - t^2}} \arctan \sinh \left(\frac{\frac{\beta \pi b}{2a}}{\sqrt{1-t^2}} \sqrt{\left(\frac{a}{b}\right)^2 + 1 - t^2} \right) dt - \\
 & - \frac{4}{\pi^2} \int_0^1 \frac{1}{\sqrt{\left(\frac{b}{a}\right)^2 + 1 - t^2}} \arctan \sinh \left(\frac{\frac{\beta \pi}{2}}{\sqrt{1-t^2}} \sqrt{\left(\frac{b}{a}\right)^2 + 1 - t^2} \right) dt,
 \end{aligned} \tag{31}$$

where

$$\beta = \frac{2\alpha a}{\pi} = \frac{a}{H} \sqrt{\frac{2-2\nu}{1-2\nu}}. \tag{32}$$

The function $F(\beta)$ describes the maximum layer bottom vertical stress $\sigma_z(0,0,H)$ by the unit uniform load acting in the rectangular region $2a \times 2b$. The depth of the influence zone is described by the point where the vertical stress due to surcharge reaches the value γh . The maximum stress below the centre of rectangle in the depth H can be then expressed in following form

$$\sigma_z(0,0,H) = f_z F(\beta) = \gamma h . \quad (33)$$

As the value of preconsolidation γh and the level of surcharge f_z are known, the value β is obtained as the inverse of the function $F(\beta)$. The following formula describes this statement and the idea how to calculate the depth of the influence zone

$$\frac{\gamma h}{f_z} = F(\beta) \rightarrow \beta = \frac{a}{H} \sqrt{\frac{2-2\nu}{1-2\nu}} \rightarrow H . \quad (34)$$

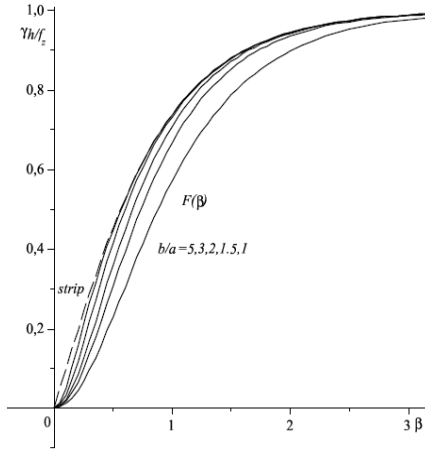


Figure 14: Courses of $F(\beta)$ function

Functions $F(\beta)$ for some quotients a/b are presented in Fig. 14.

6 FEM validation of derived formulas

The aim here is to provide results obtained from finite element analysis and compare them with results obtained from the presented theory of elastic layer. The infinite strip load was selected for comparison.

The values of $\sigma_{zz}(0, H)$ were compared. Let us first restate the derived formulas for $\sigma_{zz}(0, H)$ in the case of infinite strip load.

$$\sigma_{zz}(0, H) = \frac{2f_z}{\pi} \arctan \sinh \alpha a \quad .$$

Where: H ... depth of influence zone,
 f_z ... value of the strip load,
 ν ... Poisson's ratio,
 a ... half of the strip width,

$$\alpha \dots \alpha = \frac{\pi}{2H} \sqrt{\frac{2-2\nu}{1-2\nu}} \quad .$$

For the FEM analysis, the following assumptions were used.

- 1 degree of freedom for nodes (z – direction)
- Plain strain
- Isotropic elastic material
- Symmetry – only one half of the model
- Software ADINA (Automatic Dynamic Incremental Non-linear Analysis)

Let us note, the influences of the model width, mesh shape and type of the used finite elements (more details in [14]) were considered

The tested example has following details:

- Infinite strip load $f_z = 100000 \text{ kN/m}^2$ for $a=0,5\text{m}$; $f_z = 50000 \text{ kN/m}^2$ for $a=1,0\text{m}$; etc.
- Depth of influence zone $H = 5\text{m}$
- $E = 75 \text{ GPa}$
- ν varies from 0,05 to 0,4
- Model width $B=30\text{m}$ (15m using symmetry)

An unreal magnitude of load was used to reach sufficient digital output in the computer code.

The scheme of the example can be seen on the following figure.

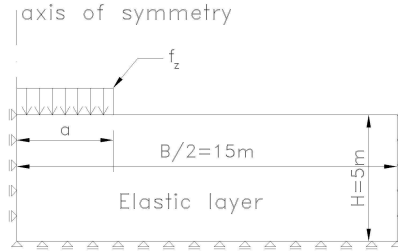


Figure 15: Scheme of the tested example

The following tables present analytical and numerical results for $a = 0\text{m} - 8\text{m}$, i.e. from line load to a very wide strip. The presented results show very good agreement. The differences are smaller than 0,1% for this range of Poisson's ratio (from 0.05 to 0.4). In all presented results, we keep the geotechnical convention in the stress values, i.e. positive stress value means pressure while the negative stress value is tension.

Table 4: Numerical results

1/2 uniform load width (m)	0	0.5	1	2	4	8
Poisson's ratio	$\sigma_{zz}(0,H)$ (kPa)					
0.05	14531.1	14412.0	14053.9	12853.8	9959.04	6044.0
0.15	15585.0	15437.8	15000.4	13565.1	10269.9	6091.8
0.25	17322.0	17118.7	16528.5	14661.8	10702.9	6147.7
0.3	18709.0	18453.2	17720.4	15472.4	10988.6	6177.8
0.35	20818.0	20464.7	19479.0	16596.9	11339.0	6207.5
0.4	24495.8	23922.6	22388.4	18273.6	11767.9	6233.1

Table 5: Analytical results

1/2 uniform load width (m)	0	0.5	1	2	4	8
Poisson's ratio	$\sigma_{zz}(0,H)$ (kPa)					
0.05	14529.7	14405.1	14049.9	12851.1	9958.2	6043.6
0.15	15583.9	15430.5	14996.2	13562.5	10269.1	6091.6
0.25	17320.5	17110.7	16524.1	14659.3	10702.4	6147.6
0.3	18708.3	18444.7	17715.8	15470.0	10988.2	6177.8
0.35	20816.7	20455.3	19474.1	16594.7	11338.6	6207.5
0.4	24494.9	23912.0	22383.3	18271.7	11767.7	6233.1

7 Conclusion

Robust theory and the derivation of many formulas were listed in the presented contribution. Much of them were numerically validated, also several tests were carried out to verify the proposed theory. There was no discrepancy found. The presented formulas will be very useful for civil engineering practice. Input parameters are very easy estimated and also they are intelligible for civil engineers. Calculation is very fast and it gives relevant results. Analytical and semi-analytical solutions significantly save time for designers contrary to pure numerical methods. Technical knowledge based on the presented theory was implemented in the computers codes, namely GEO 4, GEO 5, and FIN 10. In the details, we can list Beam, Piles, Plate, FIN 2D, FIN 3D. FINE company customers are not only large structural design companies representing the top in the world but also smaller firms taking advantage of their affordable software. Today they proudly serve more than 1300 satisfied users in more than 50 countries of the world including design and construction companies involved in many branches and also several technical universities (more information and details on www.finesoftware.eu).

ACKNOWLEDGEMENT

The research presented in this lecture has been carried out with financial support received by the author from the Contract of the Ministry of Education, Youth and Sports of the Czech Republic no. MSM 6840770001 and the Czech Science Foundation (grants no. 103/08/1119 and 103/08/1617). The author also thanks for collaboration in this research, namely to RNDr. Marii Kopáčkové, CSc., Ing. Miroslavu Broučkovi and Ing. Tomášovi Jandovi, Ph.D.

REFERENCES

- [1] Asaoka, A. , Nakano, M. and Noda, T. (1998). "Super loading yield" surface concept for the saturated structured soils", NUMGE98, edited by A. Cividini, Udine, Italy, 233-242.
- [2] Bowles, J. E. (1966), "*Foundation analysis and design*", McGraw-Hill, New York .
- [3] Cunha, R.P., Jardim, N.A. and Pereira, J.H.F. (1999). "In situ characterization of a tropical porous clay via dilatometer tests". *Geo-Congress 99 on Behaviorial Characteristics of Residual Soils*, ASCE Pub. 92, Charlotte, pp.113-122.

- [4] Cunha, R.P., Kuklík, P. (2003), “Numerical Evaluation of Pile Foundations in Tropical Soils of the Federal District of Brazil by Means of a Semi-Analytical Mathematical Procedure”
In: SOLOS E ROCHAS, SUELOS Y ROCAS, SOILS & ROCKS. 2003, vol. 26, no. 2, p. 167-182.
- [5] Daloglu, A.T., Ozgan, K. (2004), “The effective depth of soil stratum for plates resting on elastic foundation”, *Struct. Eng. Mech.*, **18**(2), 263–276.
- [6] Dluzewski, J.M. (1998), “Large strain consolidation for elastoplastic soils“, *NUMGE98*, edited by A. Cividini, Udine, Italy, 473-482.
- [7] Fajman, P., Šejnoha, J. (2007), “A simplified approach to time-dependent subsoil-structure interaction”, *Comput. Struct.*, **85**, 1514-1523.
- [8] Gradschtein, I.S., Ryzhik, I.M. (1963), *Tables of integrals, sums, series and product*, (in Russian) Moscow.
- [9] Janda, T. - Kuklík, P. - Šejnoha, M. “Mixed Experimental and Numerical Approach to Evaluation of Material Parameters of Clayey soils““In: International Journal of Geomechanics. 2004, vol. 4, no. 3, p. 199-206.
- [10]Kotrasová, K. (2009), ”Influence of category of sub-soil on liquid storage circular tanks during earthquake“
12th International Scientific Conference, Brno Czech Republic
- [11] Kuklík, P., Mares, J. and Šejnoha, M. “The structural strength of soil from the isotropic consolidation point of view“, in *APCOM 99*, Singapore, edited by C.M. Wang, K.H. Lee, K.K. Ang, 2, 797-802 (1999).
- [12] Kuklík, P., M. Kopáčeková, M. (2004), “Comparison of elastic layer solution with Boussinesq half space solution” (in Czech), *Stavební Obzor*, **6**, 171-175.
- [13] Kuklík, P. (2006) “Several Comments on Influence Zone Depth Progress in Deep Hole Foundations” *Proceedings of the GeoShanghai Conference 2006*, Reston.
- [14] Kuklík, P. - Kopáčeková, M. - Brouček, M. (2009) “Elastic Layer Theory and Geomechanics“ 1. ed. Praha: CTU Publishing House, 109 p.

- [15] Kvasnička, V. “Augmented simulated annealing adaption of feed-forward neural networks“, *Neural Network World*, **3**, 67-80 (1994).
- [16] Lewis, R.W. and Schrefler, B.A. (1998) “*The finite element method in static and dynamic deformation and consolidation of porous media*“, Wiley, Chichester, NY.
- [17] Matouš, K., Lepš, M., Zeman, J. and Šejnoha, M. (2000) “Applying genetic algorithms to selected topics commonly encountered in engineering practice“, *Comput. Methods Appl. Mech. Engrg.*, **119**, 1600-1620.
- [18] Mistrikova, Z., Jendzelovsky, N. (2009) “Soil - axisymmetric slab interaction for different models of subsoil” (in Slovak), *Civil and Environ. Eng.*, Vol.5, 2009, No.1, 18-28
- [19] Rektorys K. (1995) ”*Survey of applicable mathematics*“, ILIFFE Books, London.
- [20] Shufrin, I., Eisenberger M. (2006), “In-plane vibrations of rectangular plates with rectangular cutouts”, *Proceedings of the EPMESC X.*, Sanya (China).
- [21]Terzaghi, K., Peck, R.B. and Mesri, Ch. (1996) “Soil Mechanics in Engineering Practice”, Wiley, Chichester, NY.

Assoc. Professor Pavel Kuklík, Ph.D.

Address: CTU in Prague
Faculty of Civil Engineering
Thakurova 7, 166 29, Prague 6,
Czech Republic
Email: kuklikpa@fsv.cvut.cz

Education: doc. (Associate Prof.) CTU in Prague, Fac. of Civil
Eng., 1995
CSc. (Ph.D.) CTU in Prague, Fac. of Civil Eng., 1984
Thesis title: Solving of the Layered Subsoil.
Ing. CTU in Prague, Faculty of Civil
Engineering, Department of Geotechnics, 1975. Thesis title:
Stiffness Matrix of the Plate foundation
Individual course focused on the theory of structures, CTU in
Prague, Faculty of Civil Engineering, (1973-1975)

Professional qualification:
Teaching assistant, CTU in Prague, Faculty of Civil. Eng.,
Dept. of Struc. Mech. (1975-78}
Assistant professor, CTU in Prague, Faculty of Civil. Eng.,
Dept. of Struc. Mech. (1978-95)
Associated professor, CTU in Prague, Faculty of Civil. Eng.,
Dept. of Struc. Mech. (1995-)
Assistant professor, CTU in Prague, Faculty of Architecture,
Institute of Exact Theories (1992-95)
Visiting Professor UnB Brasília, Brazil 2001

Fields of research interest:
Constitutive modeling of soils
Foundation on piles, subsoil structure interaction
Stress measurements in site
Theory and application of the FEM
Theory and application of non-linear problems

Activity: Member of IACMAG
Member of WTA Inter
Chief of the section static and dynamic of WTA CZ

Principal investigator

GA ČR 103/98/0276, GA ČR 103/02/0688, GA ČR 103/04/1134, GA ČR 103/07/0246

and co-investigator

GA ČR 103/02/0956, GA ČR 106/05/2618, GA ČR 103/08/1617

National and international collaboration:

Fine Ltd. Na Závěrce 12, 169 00, Prague 6, Czech Republic

Ing. Jiří Laurin a Ing. Miloš Vodolan

Modeling of structures and soils, subsoil structure interaction - consulting work

Zakládání staveb a.s., K Jezu 1, 143 01 Praha 4, ČR

Ing. Milan Král, Ing. Jiří Mühl

Deep hole foundation - consulting work

UnB Brasília, Brazil

Prof. Renáto Pinto da Cunha

Pile foundations, back analysis and constitutive modeling on Brasília tropical soil

Invited lectures and short courses

Kuklík, P.

Determination of Influence Zones in Subsoils by their Structural Strength

Engenharia Civil da Universidade Federal de Goiás. 2001-11-20.

Kuklík, P.

Mixed Experimental and Numerical Approach to Evaluate the Parameters of Clayey Soil

Universidade de Brasília, Departamento de Engenharia Civil - Geotecnia. 2001-11-23.

Kuklík, P.

Shear Transfer of Pile Shafts in Collapsible Soils

Universidade de Sao Paulo, Escola de Engenharia de Sao Carlos, Departamento de Geotecnia. 2001-11-27.

Kuklík, P.

Soil-Structure Interaction Using the Winkler-Pasternak Model of Subsoil

Universidade Estadual Paulista, Faculdade de Engenharia. 2001-11-28.

Kuklík, P.
CURSO Foundation in layered subsoil 20 hours
(Visiting professor short stay UnB Brasília, Brazil) 2001

Kuklík, P.
Interaction of Subsoil and Upper Structure
University of Brasília. 2005-11-01.

Kuklík, P.
Use of Computational Tools for the Solution of Geotechnical problems Via Geo Fine Software (Tunnels, Retaining Walls and Foundations)
University of Brasília. 2005-11-01.

Kuklík, P. -Kopecký, L. - Němeček, J.
Polyethylene Terephthalate Strips as a Soil Reinforcement
University of Brasília. 2005-11-01.

Fajman, P. - Kuklík, P.
Defects of Cathedral St. Barbory in Kutna Hora
University of Brasília. 2005-11-01.

Kuklík, P. - Brouček, M.
Useful graphs and formulas for influence zone depth calculation.
University of Brasília. 2009-12-08.

Brouček, M.- Kuklík, P.
Subsoil Influenced by Groundwater Flow
University of Brasília. 2009-12-08.

Selected publications:

Cunha, R.P. - Kuklík, P.
Experimental and Numerical Analyses of Bored Pile Foundations in a Tropical Soil In: Inženýrská mechanika. 2002, vol. 9, no. 1/2, p. 91-98. ISSN 1210-2717.

Janda, T. - Kuklík, P. - Šejnoha, M.
Numerical Implementation of Isotropic Consolidation of Clayey Soils
In: Acta Polytechnica. 2003, vol. 43, no. 1, p. 8-14. ISSN 1210-2709.

- Cunha, R.P. - Kuklík, P.
Numerical Evaluation of Pile Foundations in Tropical Soils of the Federal District of Brazil by Means of a Semi-Analytical Mathematical Procedure
In: SOLOS E ROCHAS, SUELOS Y ROCAS, SOILS & ROCKS. 2003, vol. 26, no. 2, p. 167-182. ISSN 0103-7021.
- Janda, T. - Kuklík, P. - Šejnoha, M.
Mixed Experimental and Numerical Approach to Evaluation of Material Parameters of Clayey soils In: International Journal of Geomechanics. 2004, vol. 4, no. 3, p. 199-206. ISSN 1532-3641.
- Janda, T. - Cunha, R.P. - Kuklík, P. - Anjos, G.J.M.
Three Dimensional Finite Element Analysis and Back-analysis of CFA Standard Pile Groups and Pile Rafts Founded on Tropical Soils In: SOILS & ROCKS. 2009, vol. 32, no. 1, p. 3-18. ISSN 1980-7743
- Kuklík, P. - Kopáčková, M. - Brouček, M.
Fast analytical estimation of the influence zone depth, its numerical verification and FEM accuracy. Structural Engineering and Mechanics, Techno-Press 2009, vol. 33, no. 5, p. 635-647. ISSN 1225-4568
- Kuklík, P. - Šejnoha, M.
Myslenková východiska při tvorbě výpočtových modelů pro zemní tělesa
In: Geotechnika. 2000, roč. 3, č. 2, s. 27-28. ISSN 1211-913X.
- Hošek, J. - Litoš, J. - Kuklík, P. - Krejčířík, A.
Objemové změny tvrdnutí cementového pojiva v počátečním stadiu tvrdnutí betonu In: Stavební obzor. 2000, roč. 9, č. 3, s. 91-95. ISSN 1210-4027.
- Kuklík, P. - Šejnoha, M.
Kontinuální výpočtové modely pro zemní tělesa
In: Stavební obzor. 2001, roč. 10, č. 8, s. 233-237. ISSN 1210-4027.
- Kuklík, P. - Sehnoutek, L. - Masopust, J. - Mühl, J.
Statické zatěžovací zkoušky základové půdy tuhou deskou v hlubokých jamách In: Stavební obzor. 2004, roč. 13, č. 9, s. 257-260. ISSN 1210-4027.
- Kuklík, P. - Kopáčková, M.
Porovnání řešení pružné vrstvy s Boussinesqovým řešením pružného poloprostoru In: Stavební obzor. 2004, č. 6, s. 171-175. ISSN 1210-4027.

Šejnoha, M. - Kuklík, P.

Aplikace semianalytické metody a metody konečných prvků při analýze vrtaných pilot In: Geotechnika. 2006, roč. 9, č. 3, s. 3-9. ISSN 1211-913X.

Kuklík, P. - Šejnoha, M.

Interakce piloty se základovou deskou

In: Stavební obzor. 2007, roč. 16, č. 1, s. 14-19. ISSN 1210-4027.

Kopecký, L. - Němeček, J. - Kuklík, P. - Bittnar, Z. - Machovič, V.

Tranzitní zóna cementového tmelu mezi polyethylen-terftalátovou výztuží a betonem In: Stavební obzor. 2007, roč. 2007, č. 9, s. 271-273. ISSN 1210-4027.

Anjos, G.J.M. - Cunha, R.P. - Kuklík, P. - Brouček, M.

Numerical Evaluation of Bored Piles in Tropical Soils by Means of the Geotechnical Engineering "GEO4" Fine Software. In: Proceedings of III European Conference on Computational Mechanics [CD-ROM].

Lisboa: Technical University of Lisbon, 2006, ISBN 1-4020-4994-3.

Kuklík, P.

Several Comments on Influence Zone Depth Progress in Deep Hole Foundations. In: Underground Construction and Ground Movement, proceedings of the GeoShanghai Conference 2006. Reston, Virginia: ASCE, 2006, s. 355-362. ISBN 0-7844-0867-X.

Kuklík, P. - Kopáčková, M. - Brouček, M.

Elastic Layer Theory and Geomechanics 1. ed. Praha: CTU Publishing House 2009, 109 p.